Proceedings of the Korean Nuclear Society Spring Meeting
Gyeongju, Korea, 2004

Numerical Simulations on Internal Transport Barrier Formation in Reversed Shear Regime of KSTAR Tokamak

Sun Hee Kim, Jin Myung Park and Sang Hee Hong
Seoul National University

Abstract

Predictive numerical simulations on internal transport barrier formation in reversed shear regime of KSTAR tokamak have been carried out by using an ASTRA-1.5D transport code, which is coupled with a neutral beam injection code, SINBI, which have been developed in Seoul National University. In these simulations, Multi-Mode model of NTCC Library has been used as an anomalous plasma transport model and neutral beam injection is used as a main plasma heating and current drive method. It is observed from these simulations that internal transport barriers are formed in reversed shear regime and apparent in both the ion and electron temperature profiles and thermal diffusivity profiles. Simulation results also show that $\mathbf{E}\times\mathbf{B}$ flow shear and magnetic shear are responsible for the formation of internal transport barriers.

1.Introduction

Among the improvements of confinement and performance in fusion plasmas which have been reported in many tokamak devices since the 1990's, a reversed shear or negative central shear regime is the most attractive concept for preparing next generation burning plasma experiments, therefore present tokamak devices have been devoted to the study of this operation regime. In this respect, the Korea Superconducting Tokamak Advanced Research (KSTAR) tokamak also aims to reach the reversed shear operation regime[1]. The reversed shear regime is characterized by a negative or very low central magnetic shear region, where the reduced thermal transport to near neoclassical values and the reduced particle transport have been observed. The reduction of transports caused by an internal transport barrier is related with the stabilization of microturbulences by the sheared $\mathbf{E}\times\mathbf{B}$ flow and very low or negative magnetic shear suppression. Therefore, reproducing and predicting internal transport barrier through the plasma transport simulation needs a transport model based on these transport suppression physics. In this simulation work, MMM95 model[2] of National Transport Code Collaboration (NTCC) Library as a physical transport model has been used to simulate internal transport barrier formation in reversed shear regime of KSTAR tokamak. In order to produce reversed shear regime in this simulation work, neutral beam injection is used as a main plasma heating and current drive method and neutral beam heating power and driven current are calculated by a simplified neutral beam injection code (SINBI) which has been developed in Seoul National University[3]. The SINBI code includes drift orbits of fast ions to take account of the direction and losses of injected neutral beam, plasma elongation and triangularity, multi-step ionization (MSI) effect and steady-state Fokker-Planck solution to calculate the neutral beam driven current profiles. The detailed description of this SINBI code is given in reference [3]. The SINBI module is coupled with an ASTRA-1.5D transport code[4] for the simulation of the reversed shear regime of KSTAR tokamak plasma. Plasma transport suppression effects have been considered in two ways in this simulation work. The first is including an $\mathbf{E}\times\mathbf{B}$ flow shear effect in MMM95 model and the second is including a very low or negative magnetic shear effect in presence of the $\mathbf{E}\times\mathbf{B}$ flow shear effect.

2. Simulation Procedure and Transport Model

In the whole simulations of this work, plasma shape and current are assumed to increase by constant rates for the 4 seconds up to their constant saturation values. Electron and ion densities also have increased for the first 4 seconds according to the scheduled values and shapes. The electron and ion densities are determined from the reversed shear experiments of DIII-D tokamak which has a similar size with KSTAR tokamak[5]. Plasma and impurity ions are assumed as deuterium and carbon, respectively and effective charge number is set to 2.0 everywhere in the tokamak plasma. Neutral beams are injected during the current ramp-up phase to make reversed shear configuration and their powers are increased up to 10.67MW through the four time steps. Detailed KSTAR tokamak discharge parameters and neutral beam parameters are listed in Table 1 and Table 2.

Table 1. KSTAR discharge parameters for numerical simulation of reversed shear regime

KSTAR Tokamak Parameters	
Major radius R_0	1.8 m
Minor radius a	0.5 m
Triangularity δ	0.5
Elongation κ	2.0
Plasma current I	1.5 MA
Toroidal magnetic field B_0	2.5 T
Plasma ions	Deuterium
Impurity ions	Carbon
Effective charge Z_{eff}	2.0
Electron density at magnetic axis n_{eo}	4.0E19 m^{-3}

Table 2. Neutral beam parameters for numerical simulation of KSTAR tokamak reversed shear regime

Neutral Beam Parameters	
Number of beam line	2
Beam energy E_{NB}	120 keV
Beam power P_{NB}	Not fixed (MW)
E : E/2 : E/3	0.67 : 0.19 : 0.14
Beam central position (R_t, Z_t)	Beam1 : (1.8,0.0) Beam2 : (1.55,0.0)
Beam shape	Rectangular
Beam size (w, h)	(0.36, 0.70)
Gaussian half-width (σ_R, σ_Z)	(0.18, 0.35)

MMM95 model of NTCC Library, which computes plasma transport coefficients using the Multi-Mode model, has been used as a main anomalous transport model and Taroni transport model for L-mode is added by using a step function to keep the plasma edge L-mode state[6]. In addition, Galeev-Sagdeev transport model is used as a neoclassical transport model[6]. The resulting thermal diffusivities of electron and ion are as follows.

$$\chi_e = C_1\chi_e^{mmm95} + C_2 H(0.85)\chi_e^{Taroni} + C_3\chi_e^{neoclassical} \tag{1}$$

$$\chi_i = C_1\chi_i^{mmm95} + C_2 H(0.85)\chi_i^{Taroni} + C_3\chi_i^{neoclassical}, \tag{2}$$

where C_1, C_2 and C_3 are fixed to 1.0, 0.1 and 1.0, respectively. The step function $H(\rho)$ is

$$H(\rho_0) = \begin{cases} 1.0 & \rho \geq \rho_0 \\ 0.0 & \rho < \rho_0 \end{cases}, \tag{3}$$

where ρ is normalized minor radius of tokamak plasma.

The MMM95 model includes ion temperature gradient(ITG) and trapped electron mode(TEM) in the Weiland model, and resistive ballooning mode and kinetic ballooning mode. Throughout this simulation work, supershot setting of kinetic ballooning mode in the MMM95 model has been used for reversed shear regime and 10-equation version of the Weiland model has been used.

Suppression of microturbulence in tokamak plasma by the $\mathbf{E}\times\mathbf{B}$ flow shear has been considered as a suppression mechanism for tokamak plasma transport. The suppression of microturbulence occurs when the $\mathbf{E}\times\mathbf{B}$ flow shearing rate ω_S is greater than the maximum growth rate of the drift modes[7]. This effect is implemented in the MMM95 model by using the reduced growth rate $\gamma - C_S\omega_S$ in the calculation of turbulent transport coefficients. However, the level of $\mathbf{E}\times\mathbf{B}$ flow shear C_S that has to be considered to suppress plasma transport varies in accordance with tokamak devices[5] and its values has been determined by experiments up to now, therefore its transport suppression effect on KSTAR tokamak plasma has examined by varying C_S in these simulations. The shearing rate[7] is given by

$$\omega_S = \left| \frac{RB_\theta}{B_\phi} \frac{\partial}{\partial r} \left(\frac{E_r}{RB_\theta} \right) \right|, \tag{4}$$

where r, R, B_θ, B_ϕ and E_r are minor radius, major radius, poloidal magnetic field, toroidal magnetic field and radial electric field, respectively. The radial electric field is calculated from the toroidal and poloidal rotations and the ion pressure gradients[7].

$$E_r = u_{\phi i} B_\theta - u_{\theta i} B_\phi + \frac{1}{Z_i e n_i} \frac{dp_i}{dr}, \tag{5}$$

where $u_{\phi i}$ and $u_{\theta i}$ are poloidal and toroidal rotation velocities of ion, respectively. Z_i, e, n_i and p_i are ion charge number, electron charge, ion density and ion pressure, respectively. The toroidal rotation velocity is calculated simply through an assumption that total momentum transferred from neutral beam is conserved in the plasma, and the poloidal rotation velocity is obtained by using the neoclassical formula[8] embodied in the ASTRA-1.5D transport code.

The magnetic shear effect has been also included in these simulations by assuming a control function $f(s)$. The control function gives rise to strong suppression of plasma transport in the region where the magnetic shear is very low or negative. The MMM95 model includes the magnetic shear effect, but it assumes that the magnetic shear is greater than 0.5 everywhere. Therefore, very low or negative magnetic shear effect is not considered fully in this model. The control function to consider magnetic shear effect in the region of very low or negative shear is assumed as follows.

$$f(s) = \frac{1}{1 + C_m e^{-10(s-0.25)}} + \frac{1}{1 + C_m e^{10(s+0.25)}}, \tag{6}$$

where C_m is a control coefficient which determines the strength of transport suppression of magnetic shear and s is magnetic shear given by

$$s = \frac{r}{q} \frac{dq}{dr}, \tag{7}$$

where q is safety factor.

3. Simulation Results and Discussions

3.1. $\mathbf{E} \times \mathbf{B}$ Flow Shear Effect

In the first numerical simulation, $\mathbf{E} \times \mathbf{B}$ flow shear effect on plasma transport has been examined. The coefficient of $\mathbf{E} \times \mathbf{B}$ flow shear, C_S has been set to 1.0 and magnetic shear effect of very low or negative shear region is not considered. Time trace of this simulation is shown in Fig. 1. Plasma temperature and neutral beam driven current are changed in response to the change of neutral beam powers. In this simulation, normalized beta β_N (≈ 1.3) and confinement enhancement factor H_{ITER89} (≈ 1.7) are not satisfactory for advanced tokamak operation of KSTAR tokamak. In addition, bootstrap current fraction(≈ 13%) for non-inductive current drive is also insufficient due to the low plasma densities used in this simulation. However, it is thought that these values could be increased when stronger suppression of plasma transport occurs. Fig. 2 shows the radial profiles of plasma ion and electron temperatures, their thermal diffusivities, $\mathbf{E}\times\mathbf{B}$ flow shearing rate and safety factor. Ion temperature profiles show the formation of internal transport barrier related with steep gradients of ion temperature and radial expansion of it. This radial expansion is strongly related with the change of $\mathbf{E}\times\mathbf{B}$ flow shearing rate. Strong $\mathbf{E}\times\mathbf{B}$ flow shear suppression have been observed where its shearing rate ω_S is greater than 1.0×10^5/s and this effect is appeared as a reduction of thermal diffusivities of plasma ion and electron. As the peak of $\mathbf{E}\times\mathbf{B}$ flow shearing rate is shifted outward, suppression of thermal diffusivities and the steep gradients region of ion temperature are also shifted outward. When the simulation time is 4.53 second, the peak of $\mathbf{E}\times\mathbf{B}$ flow shearing rate is located at 0.3m of minor radius and suppression of ion thermal diffusivity is also appeared at that location. Formation of the very low or negative magnetic shear related with magnetic shear suppression is shown in (d) of Fig. 2 and this effect will be examined in next chapter.

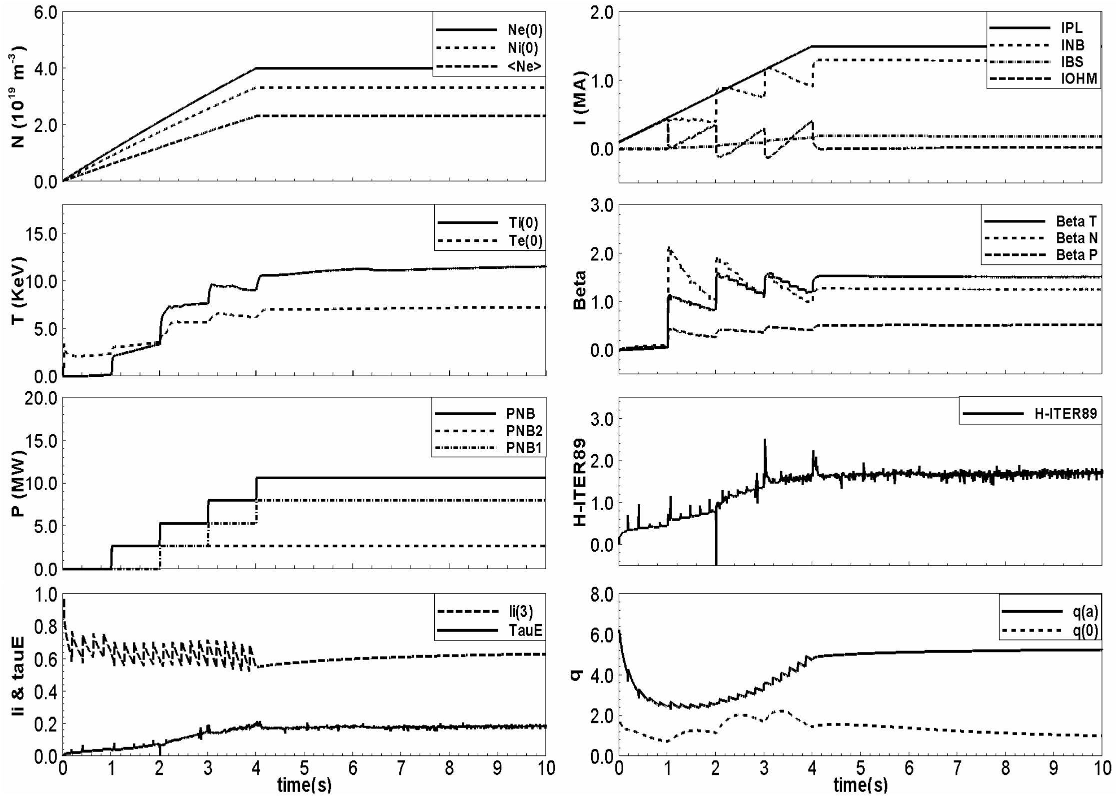

Figure 1. Time trace of the reversed shear regime simulation of KSTAR tokamak with $\mathbf{E}\times\mathbf{B}$ flow shear effect(C_S = 1.0).

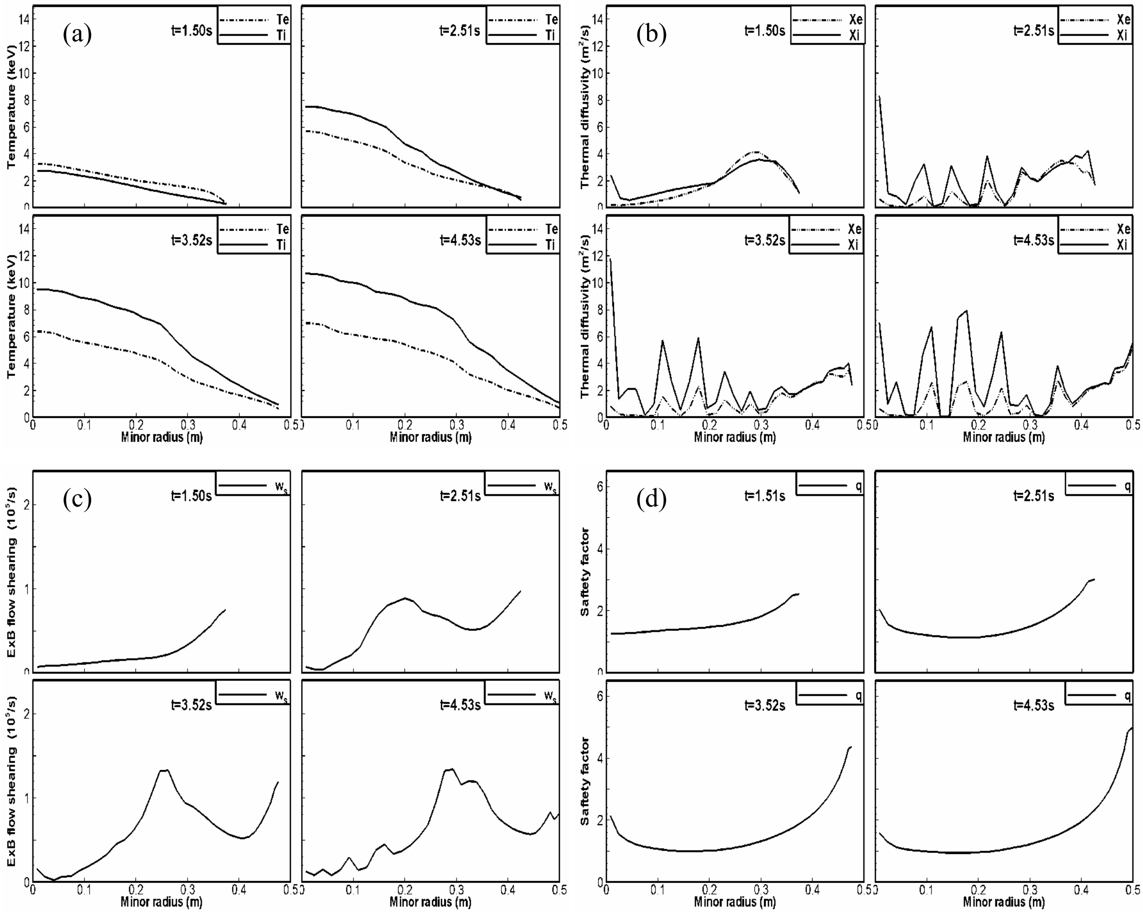

Figure 2. Radial profiles of the reversed shear regime simulation of KSTAR tokamak with $\mathbf{E}\times\mathbf{B}$ flow shear effect(C_S = 1.0). (a) electron an ion temperatures (b) thermal diffusivities of electron and ion (c) $\mathbf{E}\times\mathbf{B}$ flow shearing rate (d) safety factor

More detailed investigation of $\mathbf{E}\times\mathbf{B}$ flow shear level that has to be considered in KSTAR reversed shear regime has been carried out with no $\mathbf{E}\times\mathbf{B}$ flow shear(C_S = 0.0) and higher $\mathbf{E}\times\mathbf{B}$ flow shear(C_S = 2.0) and their radial profiles are shown in Fig.3. When the $\mathbf{E}\times\mathbf{B}$ flow shear is not considered, central ion temperature has increased to 9.4keV and transport suppression occurs inner region than the case that $\mathbf{E}\times\mathbf{B}$ flow shear is considered. When the higher level of $\mathbf{E}\times\mathbf{B}$ flow shear is considered in the MMM95 model, central ion temperature has risen to 12.3keV and transport suppression occurs outer region. In this case, both $\mathbf{E}\times\mathbf{B}$ flow shearing rate and plasma thermal diffusivities are getting stronger due to steeper ion temperature gradients, and a new state with high ion temperature is produced from a competition between the strengthened $\mathbf{E}\times\mathbf{B}$ flow shear suppression mechanism and the increased plasma thermal diffusivities. Especially, internal transport barrier is more expanded outward during the competition when higher level of $\mathbf{E}\times\mathbf{B}$ flow shear is considered.

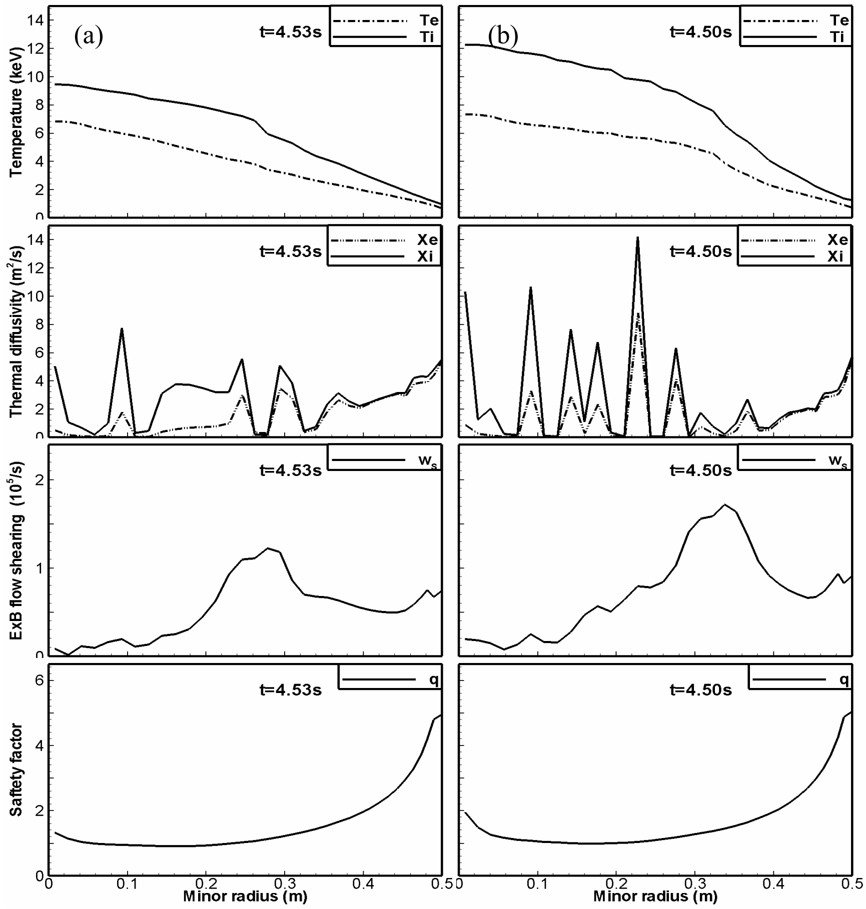

Figure 3. Radial profiles of the reversed shear regime simulation of KSTAR tokamak when (a) no $\mathbf{E}\times\mathbf{B}$ flow shear(C_S = 0.0) and (b) higher level of $\mathbf{E}\times\mathbf{B}$ flow shear(C_S = 2.0) are considered.

3.2. Magnetic Shear Effect

The very low or negative magnetic shear effect on plasma transport has been examined when lower level of magnetic shear suppression(C_m = 2.0) and higher level of magnetic shear suppression(C_m = 10.0) are considered and their simulation results are shown in Fig. 4. In both cases, plasma transport suppressions are shown in radial profiles of thermal diffusivities. In this simulation work, ion and electron thermal diffusivities are suppressed in very low and negative magnetic shear regions and therefore, central ion and electron temperatures have been strongly increased. When the magnetic shear suppression is included, central safety factor $q(0)$ is higher than the previous simulation result without the magnetic shear suppression in presence of same $\mathbf{E}\times\mathbf{B}$ flow effect as shown in (d) of Fig 2. This tendency is more obvious when the higher level of magnetic shear suppression is included as shown in (b) of Fig. 4. Especially, double peaks in $\mathbf{E}\times\mathbf{B}$ flow shearing rate profile and double steep gradient regions in ion temperature profile with central ion temperature of 15.7keV are shown in (b) of Fig. 4. In this case, confinement enhancement factor H_{ITER89} has been increased to 2.14, but bootstrap current fraction and normalized beta value have been slightly increased to 17.5% and 1.36, respectively, and it is thought that these small changes are due to the low plasma density used in this simulation.

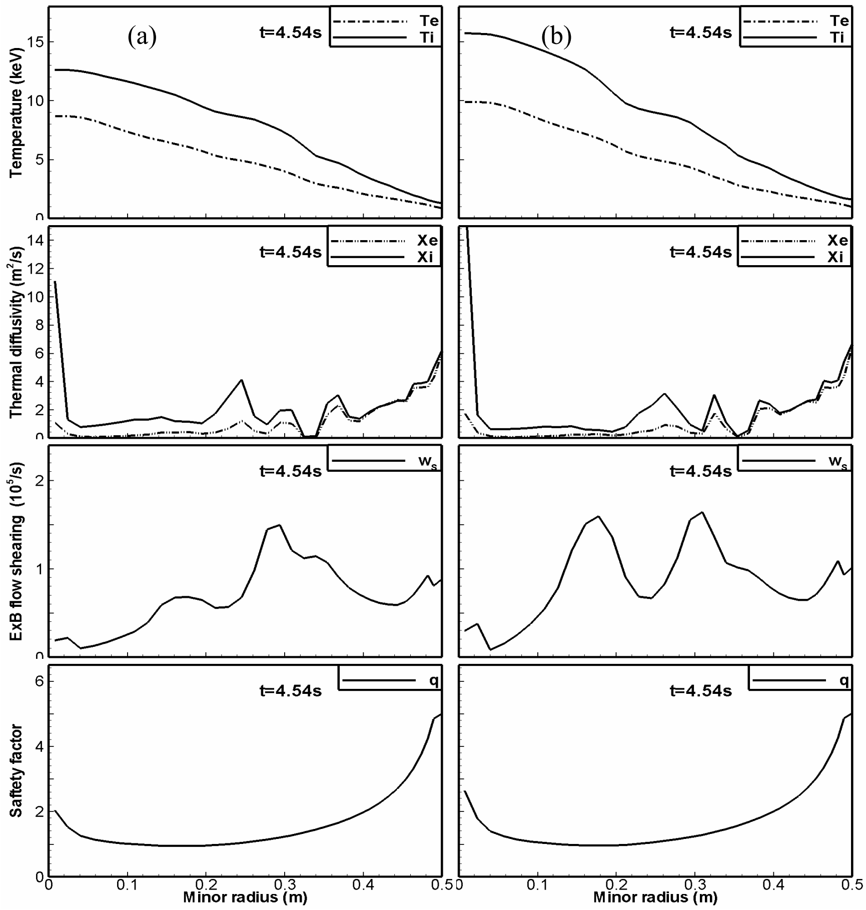

Figure 4. Radial profiles of the reversed shear regime simulation of KSTAR tokamak when (a) lower level of magnetic shear effect(C_m = 2.0) and (b) higher level of magnetic shear effect(C_m = 10.0) are considered.

4. Conclusions

In this numerical simulation work, formation of internal transport barrier in reversed shear regime of KSTAR tokamak is simulated by using the ASTRA1.5-D transport code coupled with the SINBI neutral beam injection code and the MMM95 model based on ITG and TEM physics. The internal transport barriers have appeared clearly in ion temperature profiles and ion thermal diffusivity profiles. Predicted plasma temperature profiles have steep gradients in core region of plasma and the steep gradient region has been expanded outward during the neutral beam powers are increased. The $\mathbf{E}\times\mathbf{B}$

flow shear effect on suppression of anomalous plasma transport has been examined without $\mathbf{E}\times\mathbf{B}$ flow shear and with $\mathbf{E}\times\mathbf{B}$ flow shear. Strong plasma transport suppression by the $\mathbf{E}\times\mathbf{B}$ flow shear has been occurred where its shearing rate is greater than 1.0×10^5/s and it is appeared as a reduction of thermal diffusivities of plasma ion and electron. The very low or negative magnetic shear effect is simulated by using the control function $f(s)$ in the presence of $\mathbf{E}\times\mathbf{B}$ flow shear. When the higher level of magnetic shear effect is considered, double peaks of $\mathbf{E}\times\mathbf{B}$ flow shearing rate have been observed and it suggests that magnetic shear suppression causes a synergic effect of increasing $\mathbf{E}\times\mathbf{B}$ flow shearing rate. Contribution of $\mathbf{E}\times\mathbf{B}$ flow shear effect and magnetic shear effect to the plasma transport suppression could not be determined before the KSTAR tokamak experiments, but this simulation work has shown that the internal transport barrier could simulated by using the MMM95 model based on transport suppression physics and both the $\mathbf{E}\times\mathbf{B}$ flow shear and the magnetic shear play an important role in formation of internal transport barriers. Controlling these suppression mechanisms could give some clues for advanced tokamak operation of KSTAR tokamak.

References

[1] G.S. Lee, J. Kim, S.M. Hwang, C.S. Chang, H.Y. Chang, M.H. Cho *et al*, “The KSTAR Project : An Advanced Steady State Superconducting Tokamak Experiment,” *Nuclear Fusion* **40**, 575 (2000)
[2] G. Bateman, A.H. Kritz, J.E. Kinsey, A.J. Redd and J. Weiland, “Predicting temperature and density profiles in tokamaks,” *Physics of Plasma* **5**, 1793 (1998)
[3] S.H. Kim, “Numerical Simulation on Reversed Shear Regime of KSTAR Tokamak by Neutral Beam Heating and Current Drive,” M.S. Thesis, Seoul National University, Seoul, Korea, 2004
[4] G.V. Pereverenzev and P.N. Yushmanov, “ASTRA, Automated System for Transport Analysis in a Tokamak,” *Report IPP 5/98* (2002)
[5] P. Zhu, G. Bateman, A.H. Kritz and W.Horton, “Predictive Transport Simulations of Internal Transport Barriers using the Multi-Mode model,” *Physics of Plasma* **7**, 2892 (2000)
[6] M. Ju, J. Kim, and KSTAR Team, “A Predictive Study of Non-inductive Current Driven KSTAR Tokamak Discharge Modes using a New Transport/Heating Simulation Package,” *Nuclear Fusion* **40**, 1859 (2000)
[7] R.C. Wolf, “Internal transport barriers in tokamak plasmas,” *Plasma Physics and Controlled Fusion* **45**, R1 (2003)
[8] G.M. Staebler, R.E. Waltz, and J.C. Wiley, “The Role of Rotation in Tokamak Internal Transport Barriers,” *Nuclear Fusion* **37**, 287 (1997)